Temporal variations in gaseous elemental mercury concentrations at a contaminated site: Main factors affecting nocturnal maxima in daily cycles

José M. Esbrí, Alba Martínez-Coronado, Pablo L. Higueras[*]

Instituto de Geología Aplicada, Escuela de Ingeniería Minera e Industrial de Almadén, Universidad de Castilla-La Mancha, Plaza M. Meca 1, Almadén, Ciudad Real 13400, Spain

HIGHLIGHTS

- Gaseous elemental Hg (GEM) was measured in Almadén mining district during 2 years.
- Higher daily GEM levels occurred during night hours in contaminated sites.
- Local meteorological factors appear as more relevant than photochemical processes.
- Risk assessments need to take into consideration nocturnal GEM levels.

GRAPHICAL ABSTRACT
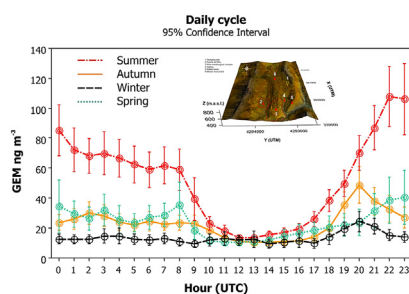
ARTICLE INFO

ABSTRACT

Mercury is considered to be a global pollutant and it has been globally transported as gaseous elemental mercury (GEM). International networks for the continuous monitoring of mercury, all of which are based on background sites, study the dispersion pattern of this metal and trends in its evolution in time and space. However, information about seasonal and daily cycling of polluted sites is scarce. The aim of the work described here was to cover this gap in knowledge. For this purpose, continuous (GEM) measurements were carried out in Almadén town from November 2011 to September 2013. Meteorological data were also collected during this time. GEM data show an average concentration during the sampling period (2011—2013) of 27.4 ng m^{-3}, with a range of 0.8—686.9 ng m^{-3}. The results highlighted seasonal and daily cycles of GEM in Almadén town, with seasonally higher levels in summer (686.9 ng m^{-3}) and significantly daily higher levels during the night. A multiple linear regression model has established wind speed as the best GEM predictor in all seasons during the night, while the best predictor in winter is relative humidity, temperature in spring, solar radiation in summer and wind speed in autumn during the day. These results provide evidence that, in mining polluted sites like Almadén, photochemical reactions have a negligible impact on GEM levels during the daytime and that meteorological parameters are more relevant. Further studies on diurnal GEM cycling in polluted sites must be carried out to obtain a realistic local risk assessment, taking into account night GEM levels and their importance in each case study.

© 2015 Elsevier Ltd. All rights reserved.

1. Introduction

Gaseous elemental mercury (GEM) is the main pollutant emitted by mercury (Hg) contaminated sites, in particular when

metallic mercury is handled. This pollutant is particularly prevalent at mining sites (Kocman et al., 2011; Kotnik et al., 2005; Higueras et al., 2013, 2014) and chlor-alkali plants using cell-Hg technology (Esbrí et al., 2015), as well as in other types of Hg-related industries (Eckley et al., 2013). The presence of high concentrations of GEM in the atmosphere may lead to uptake of this element by plants (Dago et al., 2014 and references therein) and are toxic to humans. However, such high concentrations of GEM do not affect populated areas (Higueras et al., 2013) very often and they would need to be sufficiently persistent both in quantity and over time to produce chronic effects. Tejero et al. (2015) estimated GEM concentrations in Almadén during the whole 20th Century, based on historic Hg production, and found that these concentrations must have been extremely high over long time periods. It is also important to note that the presence of GEM in the atmosphere promotes the formation of the so-called 'Reactive Gaseous Mercury' ($Hg^{2+}_{(g)}$), which returns to the surface through dry- and/or wet deposition. This species is susceptible to biological and/or physico−chemical transformations that lead to formation of organic Hg species such as methylmercury $[CH_3Hg]^+$, which is highly soluble and is able to bioaccumulate in fish and enter into the trophic chain as a pollutant (Driscoll et al., 2013).

The studied area comprises the town of Almadén and the mining and metallurgical facilities along with other minor Hg sources disseminated around the measurement location. The measurement location was located on the SSW part of Almadén (Fig. 1), some 1000 m away in the WNW direction from abandoned metallurgical facilities, which is the main source of atmospheric Hg in the area and includes an old waste dump that was restored in 2008 (Higueras et al., 2013). Other Hg sources include a restored municipal waste dump (750 m, W); an old metallurgical precinct called 'Huerta del Rey' (1200 m, NW); the mine entrance of an open gallery, now used as a ventilation gallery for the 'Almadén mining park' (700 m, WNW); and the miners monument, which is located in the center of the town and contains a considerable quantity of cinnabar (500 m, NNE). In addition to these main Hg sources, other unknown minor sources can be expected in each new building project involving contaminated soils and agricultural works on soils, especially during the ploughing of contaminated soil prior to orchard planting. All of these sources produce GEM dispersed in the Almadén atmosphere, but this does not produces in the measurement location levels up to 100 ng m^{-3} during daytime hours (centred on noon during surveys) (Higueras et al., 2013). Based on these considerations, the sampling point used in this work can be considered as corresponding to a local background area in terms of GEM levels and according to Hg distribution maps published by Higueras et al. (2013). The average total gaseous Hg level in the Almadén area during the 20th century was estimated to be 580 ng m^{-3} (Tejero et al., 2015) based on production data, but these figures are much lower today because mining and metallurgical works ceased in 2003 and the restoration of the main dump was completed in 2008. These changes in use led to a decrease in GEM levels below the most restrictive GEM alert levels (ATSDR, 1999; USEPA, 1997; WHO, 2000). One would expect that this decrease in GEM concentrations would ultimately lead to a negligible risk for the population of Almadén, but as Tejero et al. (2015) estimated, night-time levels could be two times higher than diurnal levels. The main objective of the work described here was to study in detail the seasonal and daily cycle of GEM in a polluted site like Almadén, with particular emphasis on establishing the relationships between the GEM daily cycle with meteorological conditions and their evolution over time.

2. Experimental section

Gaseous Elemental Mercury (GEM) data were collected on the top of the IGeA laboratories (WGS84 30S 340615 E/4293039 N) in Almadén (Fig. 1) from November 2011 to September 2013. The sample collector was located on a window, separated by 1 m from the building by a metal tube and at a height of 6 m above soil level, in order to avoid the effects of nearest buildings in GEM sampling. The equipment used was a Tekran 2537B device for continuous GEM measurements, with one sample of ambient air taken every 15 min. The Tekran device was calibrated every 3 days by means of an internal permeation source. An intercomparison exercise between a Lumex RA-915M and the Tekran 2537B systems was carried out during data collection in present work in conjunction with the Spanish *Instituto de Salud Carlos III* and a compatibility index (see ref. ISO/IEC, 1997) of less than 1 was found during all experiments (Fernández-Patier and Ramos-Díaz, 2011).
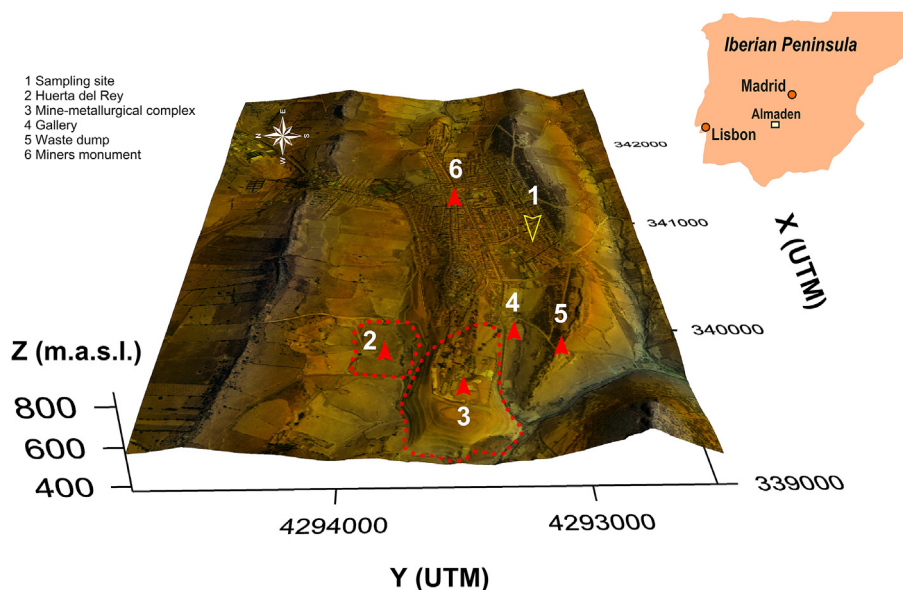

Fig. 1. Location of sampling site and main recognized Hg sources of Almadén town.

Meteorological parameters were measured, at the same time as the GEM data, on the roof of the main building of the Almadén School of Mines (WGS84 30S 340628 E/4293075N) using a dedicated Davis Vantage Pro automatic meteorological station. The main parameters measured were temperature, relative humidity, solar radiation, wind speed, wind direction, rain and barometric pressure. The study area has a Mediterranean climate with hot summers and cold winters. Average annual precipitations are in the order of 400 mm, while average temperatures range from 1 to 8 °C in January to 17–31 °C in July.

Data analysis was carried out with different software packages: Microsoft Excel, Minitab 15 and WRPlot view. All data treatment (daily cycles, seasonal statistical and multiple linear regression analysis) was performed only on data from December 2011 to November 2012. Data from November 2011 to September 2013 were only used as a reference for the year considered but was not considered for the statistical treatment because operational problems cause lost of data on this period. Daytime and night-time data were selected in relation to solar radiation cycle, avoiding sunrise and sunset periods and with seasonal differences taken into consideration. Night-time data correspond to the period 0:00–6:00 and daytime data to 10:00–16:00 in coordinated universal time (UTC).

Multiple linear regression analysis (MLRA) on the normalized dataset was carried out using Minitab 15. As a first step, a best subset regression analysis was performed to identify the best predictors using Mallows' CP. A multiple linear regression analysis was then performed on each dataset, checking that the residuals distribution was normal. A fitted line graph was constructed using the equation obtained in the MLRA and this produces another equation of the relationship between GEM measured and GEM predicted and the corresponding R^2 value.

3. Results and discussion

3.1. Seasonal and daily cycling of GEM

Measured GEM data show an average content during the sampling period (2011–2013) of 27.4 ng m^{-3} in the range (0.8–686.9) ng m^{-3}. This average GEM concentration is well above the 1.6 ng m^{-3} measured in Europe and USA as background levels (AMAP/UNEP, 2008).

Annual variations were not enough consistent, with higher levels observed during spring, summer and autumn of 2012 and winter of 2013. These variations seem to be dependent on temperature fluctuations (not reported) between these two years, but the measurement time alone is not sufficient to make any firm conclusion. The monthly evolution of these GEM contents during 2012 (see Fig. 2 for more details) shows lower concentrations during cold months (some 10 ng m^{-3} in January, February, November and December), increasing GEM levels from April to June, a GEM level reaching around 60 ng m^{-3} during summer months (June, July and August), and a decrease from August to September to the winter months. Differences between day/night GEM levels are particularly large in summer months (with night-time increase of some 60 ng m^{-3}), zero in winter months and transitional in spring and autumn months.

In a seasonal view of the data, GEM contents were higher during summer months (52 ng m^{-3} on average), in contrast to some 23 ng m^{-3} during the rest of warm seasons (spring and autumn) and 13 ng m^{-3} during winter months (Table 1). These seasonal trends are similar to those found at the *Huerta del Rey* (Fig. 1) metallurgical precinct during 2010 (Higueras et al., 2013), taking into consideration that data from 2010 were for diurnal total gaseous mercury (TGM) sampled in a regular grid on a
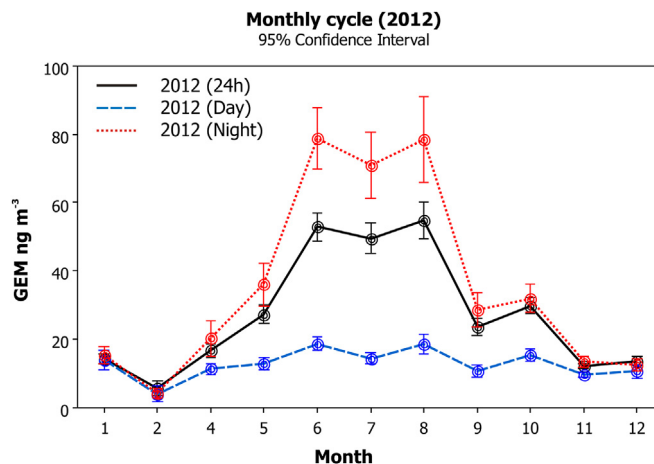

Fig. 2. Distribution of GEM levels by months and day/night hours during 2012.

contaminated area near Almadén town using a Lumex RA915M device. On the other hand, TGM data from an active facility in *Las Cuevas* mine Hg handling facility (8 km NE from Almadén) show differences in seasonal trends, with maximum GEM levels in winter during 2007, spring of 2008 and summer of 2009 (Higueras et al., 2013). It can be supposed that the main factor that affects seasonal trends in Almadén is the meteorological condition, whereas the anthropogenic factor was important in the Las Cuevas facility, where Hg handling and bottling was active during the measurement period.

Daily cycles are similar in all seasons except for winter (Table 2 and Fig. 3), with higher levels during night-time when the wind speed is lower and a certain emission capacity from soils remains. This daily pattern is the opposite to that found in remote areas far away from Hg sources, like Antarctica (Dommergue et al., 2013) or other rural areas like Wisconsin (Watras et al., 2009), where higher GEM levels are recorded at noon and are strongly dependent on temperature. The results of multiple linear regression analysis (explained in detail in Section 3.2) show that the main predictor for nightly GEM is wind speed for all seasons considered. In the studied area, the main Hg sources are the old mining and metallurgical facilities and the surrounding contaminated soils, which are widely dispersed in the vicinity of Almadén town. These two types of Hg sources had enhanced emission capacity during daytime hours due to solar radiation and higher temperatures (Llanos et al., 2011; Carmona et al., 2013) and these were responsible for the GEM levels during daytime hours. During these daily periods, solar radiation and higher temperatures promote the creation of a mixing layer in the lower tropospheric levels and this produces low and constant local winds (7 ± 3 m s^{-1}), which in turn promote dilution processes for the GEM concentrations. At dusk, when these local winds cease, maximum GEM levels are recorded in each season, reaching figures up to WHO non-recommended levels for chronic exposure, and remaining on average 5 times higher than during daytime hours in summer, two times higher in spring and autumn, and with similar figures in winter. These contrasting average GEM levels have implications for risk assessments in polluted areas and these factors have not been taken into consideration to date.

3.2. Relationships between meteorological parameters and GEM

Multiple linear regression analysis provides a better view about the influence of each meteorological factor can play on the evolution of GEM levels in a daily cycle. In this statistical treatment, only directly measured meteorological parameters were taken into

Table 1
Statistical summary of GEM levels during all sampling periods (2011−2013) and during the seasons in 2012. All data in ng m^{-3}. Abbreviations: N: number of data; Min: minimum; Max: maximum; GM: geometric mean.

	2011−2013	Winter 2012	Spring 2012	Summer 2012	Autumn 2012
N	10,870	1159	1067	2019	2025
Min	0.8	0.8	3.1	2.5	0.8
Max	686.9	122.3	279.9	686.9	281.1
Average	27.4	13.6	23.5	52.2	23.1
GM	14.1	9.0	14.6	29.0	17.5

Table 2
Statistical summary of night/day GEM levels during 2012 seasons. All GEM data in ng m^{-3}. Abbreviations: N: number of data; Min: minimum; Max: maximum; GM: geometric mean.

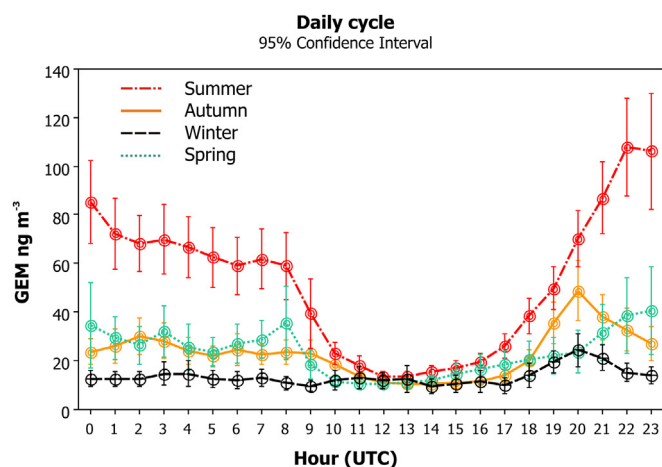|	Winter		Spring		Summer		Autumn	
	Night	Day	Night	Day	Night	Day	Night	Day
N	336	340	308	314	595	582	594	581
Min	1	1	4	3	4	2	2	1
Max	111	122	268	120	340	132	226	128
Average	13	11	28	12	69	17	26	12
GM	9	7	18	10	44	13	17	10

Fig. 3. Daily cycle of GEM levels by season.

consideration − except for wind direction, which was studied by a wind rose treatment and will be discussed later (see below). The relationships are summarized in Table 3. The clearest point is that the relevance of wind speed as a GEM predictor during night-time hours is common during all seasons, producing Pearson correlation rates between measured and predicted GEM values in a high range of 69.2−84.2%.

The main predictors during daytime hours change every season. Temperature is the best predictor in spring and, combined with relative humidity; it produces the highest R^2 (90%) (Fig. 4). Temperature and solar radiation favor soil Hg desorption by increasing Hg vapor pressure and possible photocatalytic reduction of soluble Hg^{2+} to volatile Hg^0 at the soil surface (Carmona et al., 2013). On the other hand, temperature appears to be the main factor that affects Hg emission rates in soils with high soluble Hg contents. In the transition from winter to spring, differences between maximum and minimum temperature are the highest of the year (10 °C on average and 17 °C as the highest temperature), which enhances the emission capacity of contaminated soils and dumps at Almadén and explains why temperature was the best predictor, the secondary ones being relative humidity and solar radiation. However,

in the summer season the difference between maximum and minimum temperature is 11 °C (58%), the highest increase of the seasons, while the difference between maximum and minimum solar radiation levels was 75 W m^{-2} on average (75%); so the more marked change in solar radiation conditions between spring and summer explains why solar radiation was the best predictor in the summer season. Autumn is a contrasting season since the meteorological conditions are very often changing abruptly with variations in barometric pressure and regional winds promoting wind speed, barometric pressure, relative humidity and rain as the best combined predictors during daytime hours, with a low R^2 value obtained between GEM measured and GEM predicted (70.2%). Variations in GEM levels during daytime hours were low in this season and similar to those measured in spring. However, during the spring season Hg emission-related factors act as the best predictors (temperature), whereas in autumn dilution processes seem to be predominant, with wind speed, relative humidity and rain being the best predictors. In winter, relative humidity appears to be the best predictor during daytime hours, combined with wind speed, rain and temperature, with the lowest R^2 (71.2%) of all seasons. If we consider each 15 min time period with rain as rainy period, the total rainfall in winter (23 mm/896 rainy periods) was lower than in spring (49.8 mm/1068 rainy periods) and autumn (183 mm/2008 rainy periods), but temperature and solar radiation were lower too, and the GEM levels were the lowest of all seasons. All of these factors promote rainy periods as the best predictors of small changes in GEM levels during this season (see Fig. 4 for more details).

These significant differences between daytime and night-time hours in terms of GEM emission and transport are tested in differences in R^2 between all daytime hours and night-/daytime hours, and this provides evidence that the factors affecting GEM emission and dispersion differ during different seasons and in terms of day-/night-time hours: the lowest normalized GEM levels are more apparent in night-time graphs than in diurnal ones (Fig. 4). These low levels often correspond to minor variations, which are particularly difficult to model statistically, and they produce higher R^2 values in the night-time multiple regression analysis for all seasons.

3.3. Effects of wind on higher GEM levels

In terms of the influence of wind on high or anomalous GEM concentrations, spring and autumn represent the seasons with the clearest patterns, with a narrow arc of influence centered on the main GEM source, namely the mining and metallurgical facility in Almadén (see Fig. 5 and Fig. 1 for location details). The summer pattern is quite similar, with a wider arc of influence but centered on higher GEM levels in the Westerly direction, with values similar to those corresponding to spring and summer. However, winter months show more marked differences in wind direction, with GEM levels coming from directions like NE, where only a miner's monument loaded with cinnabar is a known source in the studied area (Fig. 1): this season has the lowest GEM levels and a different

Table 3

Predictor's coefficients resulting from a multiple linear regression analysis (MLRA). The main predictors by season are shown in bold type. Abbreviations: Temp: outside temperature; Hum: outside humidity; Wind Sp.: Wind speed; Bar. Pres.: Barometric pressure; Solar Rad.: Solar radiation.

|	Constant	Temp	Hum	Wind Sp.	Bar Pres.	Rain	Solar Rad
Winter	+0.000	+0.252	+0.231	**−0.322**		+0.046	
Winter (Day)	+0.079	+0.115	**+0.301**	−0.210	−0.087	+0.117	
Winter (Night)	−0.240	+0.026	+0.167	**−0.278**	−0.003	−0.047	
Spring	+0.000	−0.018	−0.142	**−0.346**	−0.085		−0.192
Spring (Day)	−0.398	**+0.075**	+0.050	+0.019		+0.012	+0.024
Spring (Night)	−0.005		−0.013	**−0.473**	−0.095	−0.086	
Summer	+0.000	−0.070	−0.119	−0.254	−0.067		**−0.326**
Summer (Day)	+0.000	−0.044	+0.045	+0.016	+0.001		**−0.136**
Summer (Night)	+0.000	+0.014	+0.065	**−0.302**	−0.068		
Autumn	+0.008		−0.029	**−0.289**	+0.314	−0.057	−0.203
Autumn (Day)	−0.264	−0.025	+0.082	**−0.093**	+0.088	−0.086	+0.008
Autumn (Night)	+0.009	+0.074	+0.126	**−0.361**	**+0.358**	−0.067	
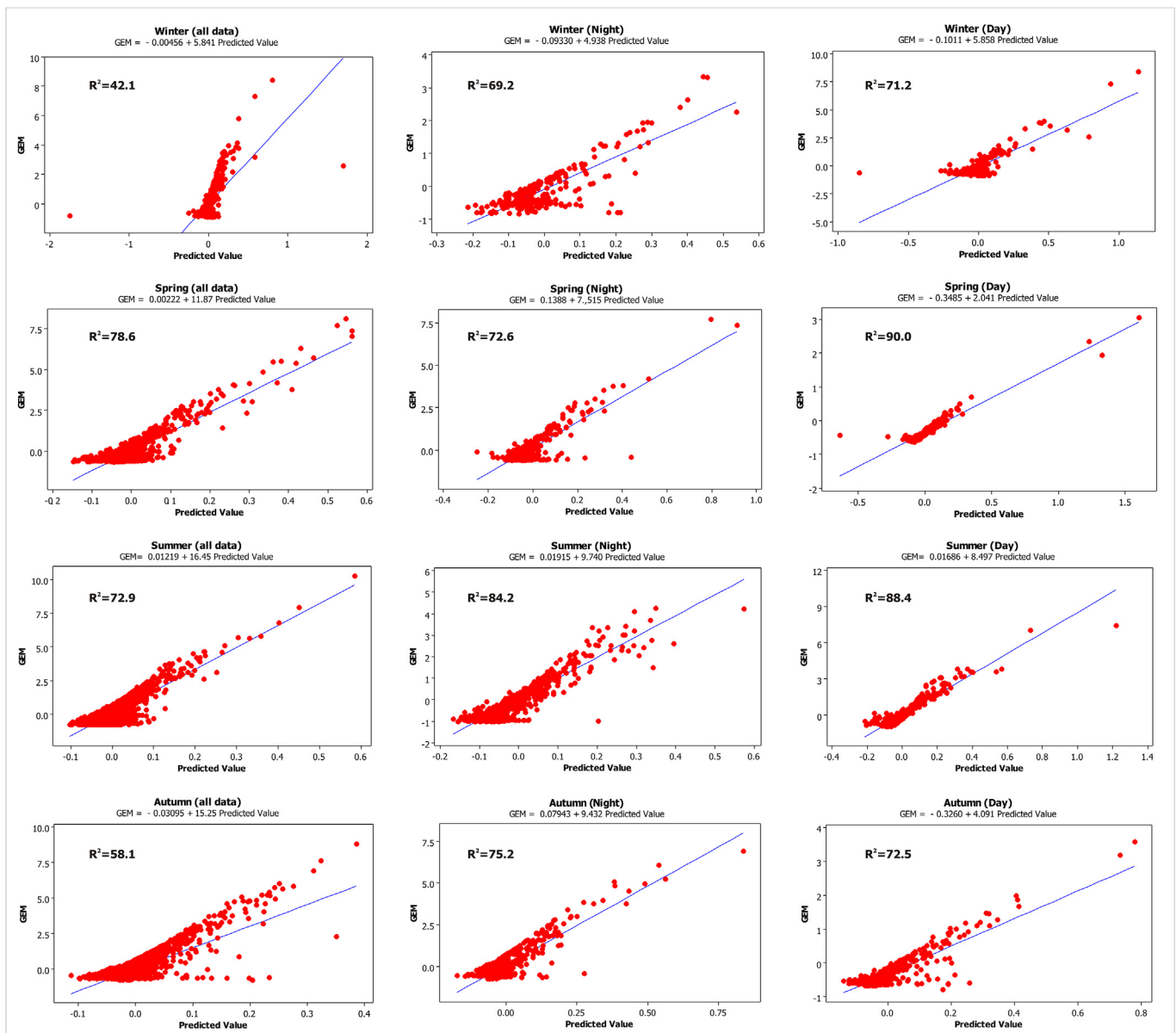
Fig. 4. Graphs of GEM measured versus GEM predicted by season and day-/night-time hours with the Pearson correlation coefficient (R^2). GEM measured and GEM predicted appear as normalized values and not as real values.
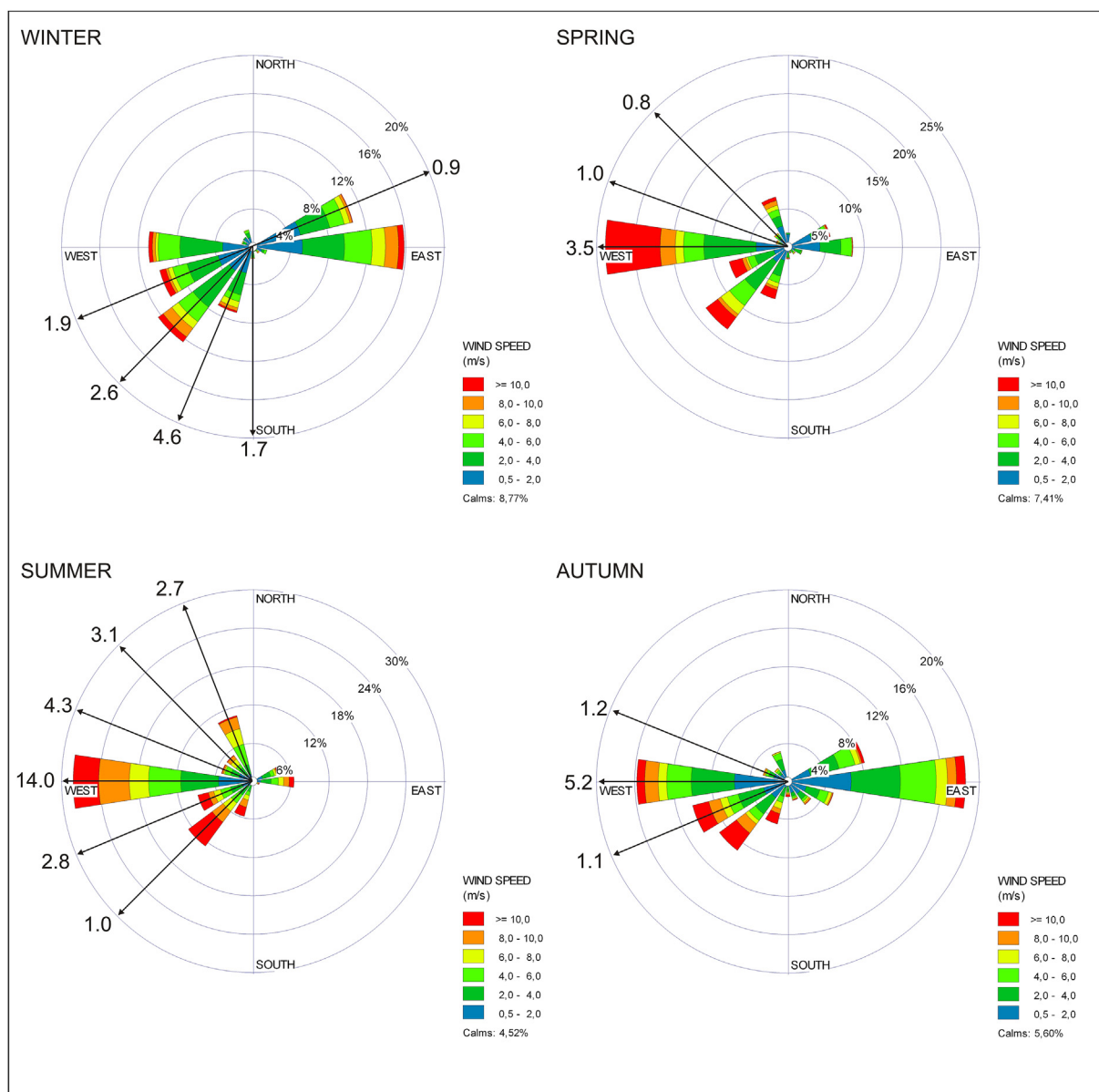
Fig. 5. Wind rose for the measurement site differenced by season. GEM levels up to 0.5 ng m^{-3} are indicated by black arrows.

wind direction pattern, and so GEM levels could be more influenced by other meteorological parameters.

3.4. Relevance of high nocturnal GEM levels in mining polluted sites

The analysis of day-/night-time GEM levels is a common topic in the recent bibliography due to its implications in emission/deposition cycles and the GEM transport mechanism (Eckley et al., 2013; Dommergue et al., 2013; Watras et al., 2009; Zhu et al., 2012; Pfaffhuber et al., 2012; Angot et al., 2014; Li et al., 2011; Kim and Kim, 2001; Stamenkovic et al., 2007). These works are systematically centered on background locations and focus on obtaining information about long range transport of GEM and other Hg species like RGM or PM. However, there is a lack of information on the behavior of GEM in contaminated areas. The data presented in this work fill this information gap by presenting GEM cycling data from the main mining and metallurgical site in Spain. These daily cycles reach maximum levels during night-time hours, when the soil

emission capacity and especially the wind speed are lower; this is in many cases the opposite to the case in rural or urban areas with low-grade contamination, where maximum levels are recorded at noon or in diurnal hours (Eckley et al., 2013; Dommergue et al., 2013; Watras et al., 2009; Zhu et al., 2012) or a non-diurnal pattern was found (Pfaffhuber et al., 2012; Angot et al., 2014). Diurnal patterns such as the one found in this work were only reported in background sites from China (Li et al., 2011) and Seoul (Kim and Kim, 2001). Li et al. (2011) explained these higher nocturnal GEM levels as being due to photochemical reactions with O_3, OH radicals and reactive halogen species, combined with differences in air-temperature during daytime hours and the creation of a mixing layer during daytime hours. This process dilutes GEM, with GEM captured and concentrated during night-time hours when this mixing layer disappears. These possibilities could explain the high GEM levels observed during the night in background areas, where GEM levels are generally below 3 ng m^{-3}. However, at polluted sites like Almadén town, where the average GEM levels are

around 27 ng m^{-3}, meteorological conditions appear to be the main factors involved in the creation of diurnal cycles and photochemical reactions are unimportant in explaining these changes in concentrations. Stamenkovic et al. (2007) reported a daily cycle that was quite different, with higher levels in the mid-morning and lower levels in the afternoon. The authors hypothesized, in a similar way to Li et al. (2011), that atmospheric oxidants could be involved in the diurnal cycle in combination with the creation of a mixing layer. In Almadén town, the diurnal cycle (Fig. 2) has its maximum level at dusk due to the disappearance of the mixing layer, when contaminated soils still have a high enough capacity to emit Hg. This soil emission is predominantly temperature dependent (Carmona et al., 2013) and produces higher average GEM levels during night-time hours in summer. Deposition rates seem to be predominant only in autumn months, when rain appears to be one of the best predictors of daytime GEM levels.

4. Conclusions

Seasonal and diurnal cycles of GEM in a mining contaminated site show maximum levels on summer months and nocturnal hours. The MLRA provide evidence that different factors control this GEM levels on each season: relative humidity in winter, temperature in spring, solar radiation in summer and wind speed in autumn, while wind speed appears as the main factor involved in higher nocturnal levels. This fact has significant influence on risk assessment in contaminated sites such as mining or industrial areas that have been evaluated based only on diurnal atmospheric Hg measurements. In these risk assessments, however, it was not considered that, in the surroundings of polluted sites, daily trends of ambient Hg could be similar to trends described in this work in Almadén town, with high Hg concentrations in soils, a high emission capacity linked with temperature and solar radiation, and a high accumulation capacity on the boundary layer linked to low wind speed during the night. This scenario must be taken into account in future risk assessments of polluted sites. In this sense, greater effort should be directed towards continuous Hg measurements in polluted sites in order to achieve a better understanding of daily cycling, especially in transition hours at dawn or dusk, when meteorological factors like air temperature, soil temperature, solar radiation and wind speed could be more influential than photochemical transformations or emission/deposition cycles.

References

AMAP/UNEP, 2008. Technical Background Report to the Global Atmospheric Mercury Assessment. Arctic Monitoring and Assessment Program/UNEP Chemical Branch, 159 pp. A logical Profile for Mercury. Agency for Toxic Substances and Disease Registr, U.S. http://www./hazardoussubstances/Mercury/MercuryPublications/GlobalAtmosphericMercuryAssessmentSourcesErn/tabid/3618/Default.aspx http://www.atsdr.cdc.gov/toxprofiles/tp46.html (accessed 04.12).

Angot, H., Barret, M., Magand, O., Ramonet, M., Dommergue, A., 2014. A 2-year record of atmospheric mercury species at a background southern hemisphere station on Amsterdam Island. Atmos. Chem. Phys. 14 (20), 11461–11473.

ATSDR, 1999. Toxicological Logical Profile for Mercury. Agency for Toxic Substances and Disease Register, U.S, pp 509. http://www.atsdr.cdc.gov/toxprofiles/tp46.pdf (accessed 17.03.15).

Carmona, M., Llanos, W., Higueras, P., Kocman, D., 2013. Mercury emissions in equilibrium: a novel approach for the quantification of mercury emissions from contaminated soils. Anal. Methods 5 (11), 2793–2801.

Dago, A., González, I., Ariño, C., Martínez-Coronado, A., Higueras, P., Díaz-Cruz, J.M., Esteban, M., 2014. Evaluation of mercury stress in plants from the Almadén mining district by analysis of phytochelatins and their Hg complexes. Environ. Sci. Technol. 48 (11), 6256–6263.

Dommergue, A., Vogel, N., Ferrari, C.P., Magand, O., Barret, M., 2013. Preliminary Results from a Continuous Record of Atmospheric Gaseous Mercury at the Coastal Station Dumont d'Urville in Antarctica. E3S Web of Conferences 1, No27005.

Driscoll, C.T., Mason, R.P., Chan, H.M., Jacob, D.J., Pirrone, N., 2013. Mercury as a global pollutant: sources, pathways, and effects. Environ. Sci. Technol. 47 (10), 4967–4983.

Eckley, C.S., Parsons, M.T., Mintz, R., Lapalme, M., Mazur, M., Tordon, R., Elleman, R., Graydon, J.A., Blanchard, P., St Louis, V., 2013. Impact of closing Canada's largest point-source of mercury emissions on local atmospheric mercury concentrations. Environ. Sci. Technol. 47 (18), 10339–10348.

Esbrí, J.M., López-Berdonces, M.A., Fernández-Calderón, S., Higueras, P., Díez, S., 2015. Atmospheric mercury pollution around a chlor-alkali plant in Flix (NE Spain): an integrated analysis. Environ. Sci. Pollut. Res. 22, 4842–4850.

Fernández-Patier, R., Ramos-Díaz, M.C., 2011. Informe del Ejercicio de Intercomparación de Mercurio Gaseoso total en aire ambiente "IN SITU" (año 2011). Ined. Repport, Instituto de Salud Carlos III, Centro Nacional de Sanidad Ambiental, Área de Contaminación Atmosférica. Ministerio de Economía y Competitividad, España.

Higueras, P., Esbrí, J.M., Oyarzun, R., Llanos, W., Martínez-Coronado, A., Lillo, J., López-Berdonces, M.A., García-Noguero, E.M., 2013. Industrial and natural sources of gaseous elemental mercury in the Almadén District (Spain): an updated report on this issue after the cease of mining and metallurgical activities in 2003 and major land reclamation works. Environ. Res. 125, 197–208.

Higueras, P., Oyarzun, R., Kotnik, J., Esbrí, J.M., Martínez-Coronado, A., Horvat, M., López-Berdonces, M.A., Llanos, W., Vaselli, O., Nisi, B., Mashyanov, N., Ryzov, V., Spiric, Z., Panichev, N., McCrindle, R., Feng, X., Fu, X., Lillo, J., Loredo, J., García, M.E., Alfonso, P., Villegas, K., Palacios, S., Oyarzún, J., Maturana, H., Contreras, F., Adams, M., Ribeiro-Guevara, S., Niecenski, L.F., Giammanco, S., Huremović, J., 2014. A compilation of field surveys on gaseous elemental mercury (GEM) from contrasting environmental settings in Europe, South America, South Africa and China: separating fads from facts. Environ. Geochem. Health 36 (4), 713–734.

ISO/IEC Guide 43-1, 1997. Proficiency Testing by Interlaboratory Comparisons Part 1: Development and Operation of Laboratory Proficiency Testing. http://www.iso.org/iso/iso_catalogue/catalogue_tc/catalogue_detail.htm?csnumber=27216 (accessed 18.03.15).

Kim, K., Kim, M., 2001. The temporal distribution characteristics of total gaseous mercury at an urban monitoring site in Seoul during 1999-2000. Atmos. Environ. 35 (25), 4253–4263.

Kocman, D., Vreča, P., Fajon, V., Horvat, M., 2011. Atmospheric distribution and deposition of mercury in the Idrija Hg mine region, Slovenia. Environ. Res. 111 (1), 1–9.

Kotnik, J., Horvat, M., Dizdarevič, T., 2005. Current and past mercury distribution in air over the idrija Hg mine region, Slovenia. Atmos. Environ. 39 (39), 7570–7579.

Li, Z., Xia, C., Wang, X., Xiang, Y., Xie, Z., 2011. Total gaseous mercury in Pearl River delta region, China during 2008 winter period. Atmos. Environ. 45 (4), 834–838.

Llanos, W., Kocman, D., Higueras, P., Horvat, M., 2011. Mercury emission and dispersion models from soils contaminated by cinnabar mining and metallurgy. J. Environ. Monit. 13, 3460–3468.

Pfaffhuber, K.A., Berg, T., Hirdman, D., Stohl, A., 2012. Atmospheric mercury observations from Antarctica: seasonal variation and source and sink region calculations. Atmos. Chem. Phys. 12 (7), 3241–3251.

Stamenkovic, J., Lyman, S., Gustin, M.S., 2007. Seasonal and diel variation of atmospheric mercury concentrations in the Reno (Nevada, USA) airshed. Atmos. Environ. 41 (31), 6662–6672.

Tejero, J., Higueras, P., Garrido, I., Esbrí, J.M., Oyarzun, R., Español, S., 2015. An estimation of mercury concentrations in the local atmosphere of Almadén (Ciudad Real Province, South Central Spain) during the twentieth century. Environ. Sci. Pollut. Res. 22, 4833–4841.

USEPA, 1997. Mercury Study Report to Congress (Volume V: Health Effects of Mercury and Mercury Compounds). EPA-452/R-97-007V. United States Environmental Protection Agency, Washington DC, USA. www.epa.gov/hg/report.htm (accessed 18.03.15) 349 pp.

Watras, C.J., Morrison, K.A., Rubsam, J.L., Rodger, B., 2009. Atmospheric mercury cycles in northern Wisconsin. Atmos. Environ. 43, 4070–4077.

WHO, 2000. Air Quality Guidelines for Europe. WHO Regional Publications European Series 91. World Health Organization Regional Office for Europe, Copenhagen, 288 pp.

Zhu, J., Wang, T., Talbot, R., Mao, H., Hall, C.B., Yang, X., Fu, C., Zhuang, B., Li, S., Han, Y., Huang, X., 2012. Characteristics of atmospheric total gaseous mercury (TGM) observed in urban Nanjing, China. Atmos. Chem. Phys. 12 (24), 12103–12118.